Highlights of Spanish Astrophysics XII, Proceedings of the XVI Scientific Meeting of the Spanish Astronomical Society held on July 15 - 19, 2024, in Granada, Spain. M. Manteiga, F. González Galindo, A. Labiano Ortega, M. Martínez González, N. Rea, M. Romero Gómez, A. Ulla Miguel, G. Yepes, C. Rodríguez López, A. Gómez García and C. Dafonte (eds.), 2025

Exploring Emerging Ionized Regions of Pre-Planetary Nebulae: An ALMA Close-Up

Sánchez Contreras, C.[1], Tafoya, D.[2], Fonfría, J.P.[3], Alcolea, J.[3], Castro-Carrizo, A.[4], and Bujarrabal, V.[4]

[1] Centro de Astrobiología (CAB), CSIC-INTA, ESAC-campus, Camino Bajo del Castillo s/n, E-28692, Villanueva de la Cañada, Madrid, Spain.
[2] Department of Space, Earth, Environment, Chalmers University of Technology, Onsala Space Observatory, 439 92 Onsala, Sweden
[3] Observatorio Astronómico Nacional (OAN), IGN, Alfonso XII No 3, 28014 Madrid, Spain
[4] Institut de Radioastronomie Millimetrique, 300 rue de la Piscine, 38406 Saint Martin d'Heres, France

Abstract

We present recent results from our successful and pioneering observational program with the Atacama Large Millimeter/submillimeter Array (ALMA) to study emerging ultracompact HII regions in pre- and young-Planetary Nebulae (pPNe/yPNe). By utilizing mm-wavelength recombination lines (mm-RRLs) as novel tracers, we have gained unprecedented insights into the inner workings of these fascinating objects. This project is innovative in two significant ways. First, it focuses on the challenging task of characterizing the core regions of pPNe, which remain largely unexplored in most cases. Second, it employs mm-RRLs as unconventional tracers: although these lines are exceptional for probing the deep core regions of pPNe, they have seen limited use due to their intrinsic weakness. This talk focuses on our detailed study of the iconic pPN/yPN M 2-9. With an angular resolution down to $\sim$30 mas ($\sim$20 au at d=650 pc), we unveil the structure and kinematics of its elusive inner nebular regions (within $\sim$100 au). The ionized central region of M 2-9 is elongated along the symmetry axis of its large-scale nebula, consistent with a collimated bipolar wind (or *jet*), and exhibits axial velocity gradients with expansion speeds up to $\sim$80 km s^{-1}. Time variability in the intensity and width of the H30α and H39α line profiles is also observed, indicating physical and kinematic changes of the jet over a few years. Using the new 3D non-LTE radiative transfer code Co^{3}RaL, we model these observations in detail, shedding light on the physical conditions in the inner regions, key to understand the development of asymmetries in pPNe.

1 Introduction

Pre-planetary nebulae (pPNe) are in the transitional phase between the asymptotic giant branch (AGB) and planetary nebula (PN) stages in the evolution of low-to-intermediate mass stars (0.8-8 $M_{\odot}$), marking their final luminous stages before becoming white dwarfs (WDs). During the AGB phase, significant mass loss occurs through a dense, slow ($\sim$5-30 km s^{-1}) wind that forms a circumstellar envelope (CSE) around the star [8]. As this mass loss stops, the stars evolve into the post-AGB or pPN phase and eventually into PNe, with the central star heating up to ionize the previously expelled material. This rapid AGB-to-PN transition ($\approx$1000 years) limits our understanding of pPNe [9]. A key question is how spherical, slowly expanding AGB envelopes transform into non-spherical PNe with fast outflows ($\sim$100 km s^{-1}). PNe exhibit diverse morphologies—elliptical, bipolar, multipolar—with substructures like jets and bright knots ([15, 18]). Studies suggest this shaping begins in the late AGB or early post-AGB phases, making pPNe crucial for understanding the formation of PNe and their early evolution ([14, 3]).

The mechanisms behind PNe shaping are still debated. It is thought that fast, collimated jets interacting with the AGB wind create shocks that shape the CSE [1]. Binaries and magnetic fields are likely responsible for launching these jets, but direct observation of post-AGB jets and their launch regions is difficult due to their small size and heavy obscuration by circumstellar dust. A recent pilot study using mm-RRLs has proven effective in probing deeply into ionized regions within $\sim$150 au, allowing for better insight into jet formation and ongoing post-AGB mass-loss rates [16]. This study detected mm-RRLs in three objects—MWC 922, M 2-9, and CRL 618—offering the first detailed look at their central ionized regions. For M2-9 and CRL 618, data showed young ($\lesssim$15-20 years) bipolar outflows with moderate velocities (tens of km s^{-1}) and high mass-loss rates ($\sim 10^{-7}$-10^{-6} $M_{\odot}$ yr^{-1}). In MWC 922, an IR-excess B[e]-type star with an X-shaped reflection nebula, line profiles suggested a rotating disk and a wind. Later ALMA observations by [17] confirmed a nearly edge-on rotating disk and revealed a fast ($\sim$100 km s^{-1}) bipolar wind aligned with the disk's rotation axis.

To obtain a better characterization of the central ionized cores of M 2-9, and CRL 618, we carried out interferometric observations with ALMA. This contribution outlines our study of M 2-9. This iconic well-studied yPN candidate (e.g. [6, 4, 5, 16, 2]) has prominent large-scale lobes oriented in a north-south direction, exhibiting significant expansion dynamics. Indirect, yet compelling evidence indicates the presence of a binary system with an estimated orbital period of $\sim$90 yr, though the specific characteristics of this system remain unclear. Radio continuum emission has been detected ([10, 11, 7]), particularly from a compact central region (of radius $\lesssim 0\farcs2$), indicating an ionized wind from the core, which is the focus of the current study.

2 Observations

The observations were conducted using the ALMA 12-m array as part of projects 2016.1.00161.S and 2017.1.00376.S. The observations were carried out in Band 3 (3 mm) and Band 6 (1 mm), with a total of twelve different spectral windows (SPWs) dedicated to mapping the emission

of various mm-RRLs (and CO lines) as well as the continuum. Observations were conducted in October and November 2017 using 45-50 antennas, with baselines ranging from 41.4 m to 16.2 km for Band 3, and from 113.0 m to 13.9 km for Band 6. The maximum recoverable scale (MRS) of the observations is $\sim$0.″8 and $\sim$0.″7 at 3 and 1 mm, respectively. Full details on the observations and imaging techniques can be found in Sánchez Contreras et al., in preparation. The final mm-RRL cubes and continuum maps presented here have angular resolution of $\sim$30-40 mas at 1 mm and $\sim$40-80 mas at 3 mm.

3 Results

3.1 An ionized bent jet surrounded by a circumbinary disk

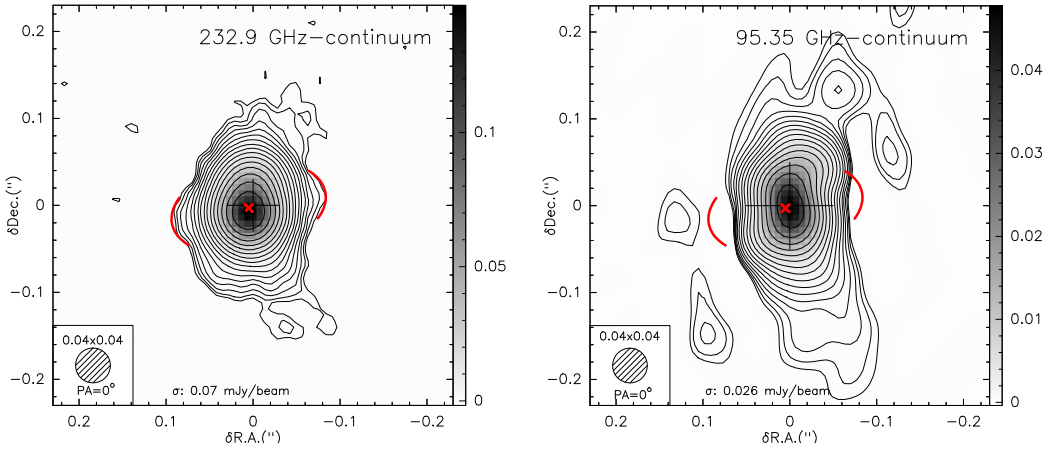

Figure 1: ALMA continuum emission maps of M 2-9 at 232.9 GHz (left) and 95.4 GHz (right) using a circular restoring beam with half power beam width of HPBW=0.″04. The level contours are $(3\sigma)\times1.5^{(i-1)}$ Jy beam^{-1}, i=1,2,3... The central cross marks the 3 mm continuum peak at coordinates J2000 R.A.=$17^{\rm h}05^{\rm m}37\overset{\rm s}{.}97$ and Dec.=$-10°08'32\overset{''}{.}65$ (J2000). The red arcs represent the broad-waist structure, plausibly a dust disk.

The ALMA continuum maps at 1 and 3 mm (Fig. 1), show an elongated structure that resembles what is seen at longer wavelengths. At 3 mm, we discern a C-shaped curvature similar to that observed in 2015 in the VLA 7 mm maps [7] consistent with a bent collimated wind (jet) emerging from the core. This jet has dimensions of 0.″4×0.″13 (260×85 au at 650 pc, [4]) at 3 mm. We measure a spectral index of the continuum of $S_\nu \propto \nu^{0.92\pm0.10}$, which suggests predominantly free-free emission from the ionized jet, with a minor contribution from dust.

There are some differences between the 1 mm and 3 mm maps that partly arise from the frequency-dependence of the free-free continuum optical depth and from the increased contribution of thermal dust emission to the continuum at shorter wavelengths. In particular, the 1 mm maps show a broad-waist of emission, absent at 3 mm and in the mm-RRLs maps, which very likely represents a dusty equatorial disk (with a radius of $\sim$50 au) surrounding

the ionized jet. This mm-continum disk is probably the counterpart of the compact, dust disk known to exist at the core of M 2-9 based on mid-infrarred observations [13].

Further support for the existence of an equatorial disk around the ionized jet comes from our observation of a CO compact absorption that is slightly offset to the north (by $\sim$0.″012) from the center (not shown). Considering the system's inclination, with the north lobe oriented at an angle of $i\sim17^\circ$ away from the plane of the sky, this offset is in line with the absorption of the background free-free continuum (from the ionized core) occurring by the front part of an equatorial disk. The CO absorption feature is redshifted by $\sim$6 km s^{-1} from the centroid of the mm-RRLs, which is most likely due to infall motions from the inner regions of the circumbinary disk.

3.2 Kinematics of the ionized jet

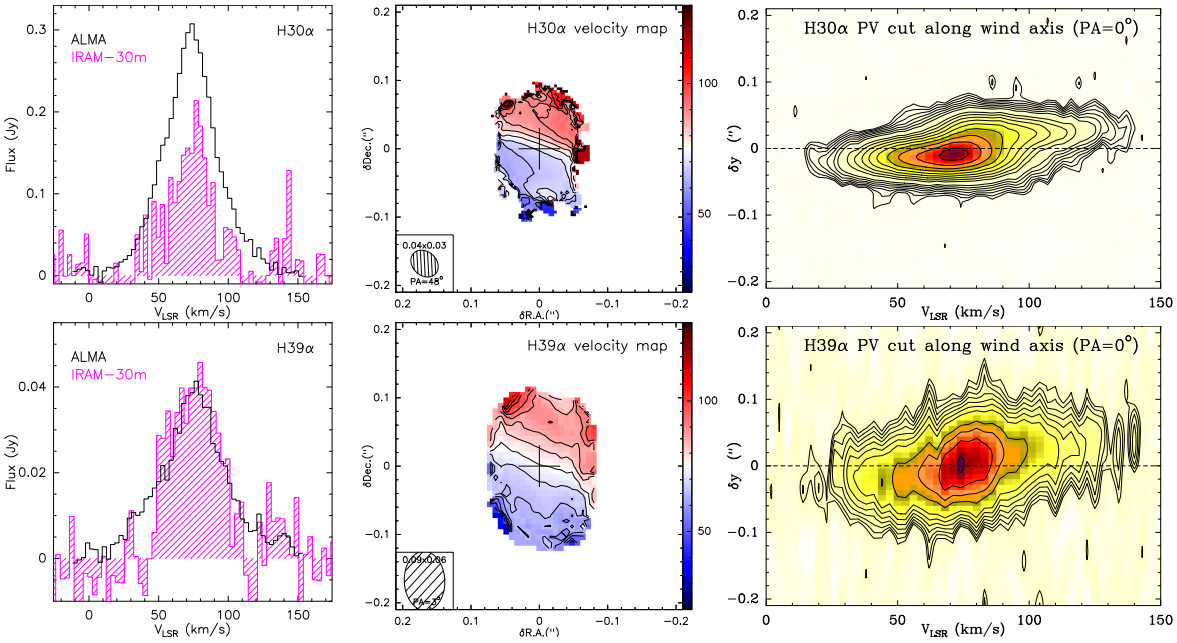

Figure 2: Summary of ALMA data of the H30α (top) and H39α (bottom) recombination lines. Left: Integrated line spectrum obtained with ALMA (black lines) and with the IRAM-30 m antenna (pink histogram, [16]). Middle: First moment map. Contours going from $V_{\rm LSR}$=45 to 115 km s^{-1} by 5 km s^{-1}. The wedge indicates the $V_{\rm LSR}$-color relationship. Right: Position velocity cuts through the center along the wind axis (PA=0°). Levels are $2.5\times(1.\ 3)^{(i-1)}$ for H30α and $1.5\times(1.3)^{(i-1)}$ for H39α with i=1,2,3...

As shown in Fig. 2, the H30α and H39α line emission span a wide velocity range of $\sim$140 km s^{-1}, sharing a similar extent and morphology with the mm-continuum emission (with the exception of the broad waist at 1 mm). The comparison between the ALMA line profiles (integrated over the emitting area) with those obtained 2 years earlier with the IRAM-

30 m antenna [16] shows that the lines are now more intense and broader, implying changes of the wind properties over yearly time scales.

The ionized jet's kinematics can be examined using the moment-1 maps and position-velocity diagrams. We observe a global expansion indicated by an overall velocity gradient along the nebula's symmetry axis (PA=0°). The velocity gradient suggests very short kinematical ages of less than approximately one year, consistent with the observed changes in the line profiles over the course of a year. Additionally, we note a slight velocity gradient perpendicular to the lobes, which is evident in the sloping (non-horizontal) isovelocity contours in the momentum-1 map, tentatively suggesting jet rotation. The axial position-velocity diagrams display a distinctive S-shape, showing maximum line widths at two compact regions located diametrically opposed along the axis (at offsets of ∼20-30 mas), indicating either rapid/abrupt wind acceleration or shocks at these compact regions (referred to as "HVspots").

3.3 Non-LTE radiative transfer modeling

For a comprehensive analysis of the spatio-kinematics and physical conditions of the ionized jet, we are currently conducting radiative transfer modeling using the Co^{3}RaL code (Sánchez Contreras et al., in prep). Although the modeling is ongoing, it appears that a wind with a non-uniform density structure is necessary to account for the observations. Notably, the HVspots are well depicted by two regions of high-density and high-velocity, resembling the shock-compressed bipolar structure proposed by [12] in their model for M 2-9, which is based on the interaction of a tenuous companion-launched jet and the dense primary star's wind. We find an average electron temperature of $T_{\rm e}$∼15,000 K and densities ranging from $n_{\rm e}$≈10^6 to 10^8 cm^{-3}. The average mass-loss rate of the ionized jet is of $\dot{M}$≈10^{-7} $M_\odot$ yr^{-1}.

4 Conclusions

In this presentation, we highlight the importance of mm-RRLs to investigate the intriguing central ionized regions of pPNe, specifically of M 2-9. Observations with the ALMA-12m array of these lines, along with the free-free continuum, provide a unique opportunity to closely examine the jet engine and estimate the mass-loss rate associated with ongoing ejections. Here is a summary of some of our findings for the iconic pPN/yPN M 2-9:

- The mm-continuum emission shows a ∼260×85 au structure elongated along the symmetry axis of the large-scale bipolar nebula, consistent with an ionized bent jet.
- Evidence for a compact equatorial disk of radius ∼50 au perperdicular to the jet is found in the 1 mm-continuum maps, and is supported by observed redshifted CO absorption profiles, indicating gas infall movements from the disk toward a central source.
- The mm-RRLs display velocity gradients along the axis, implying systematic expansion within the jet, with peak expansion velocities of ∼80 km s^{-1} observed in compact regions (HV spots).
- A subtle velocity gradient perpendicular to the lobes suggests rotational motions in the jet ($V_{\rm rot}$∼7-10 km s^{-1}).

- Our ALMA observations reveal increased brightness and width in the mm-RRLs compared to prior observations, indicating variations in wind kinematics and physical conditions on timescales of less than two years.
- Radiative transfer modeling indicates an average electron temperature of $T_{\rm e}$∼15,000 K and a non-uniform density structure within the ionized wind, with electron densities ranging from $n_{\rm e}$≈10^6 to 10^8 cm^{-3}. The mass and average mass-loss rate of the ionized jet is $M_{\rm ion}$∼$4\times10^{-6}\,M_\odot$ and $\dot{M}$≈$10^{-7}\,M_\odot$ yr^{-1}, respectively.
- These findings suggest a complex bipolar structure resulting from the interaction between a tenuous companion-launched jet and the dense wind of the primary star.

Acknowledgments

We acknowledge funding from the Spanish MCIN/AEI/10.13039/501100011033 (projects PID2019-105203GB-C22 and PID2019-105203GB-C21). This paper makes use of the following ALMA data: ADS/JAO.ALMA#2016.1.00161.S and ADS/JAO.ALMA#2017.1.00376.S. ALMA is a partnership of ESO (representing its member states), NSF (USA) and NINS (Japan), together with NRC (Canada), MOST and ASIAA (Taiwan), and KASI (Republic of Korea), in cooperation with the Republic of Chile. The Joint ALMA Observatory is operated by ESO, AUI/NRAO and NAOJ.

References

[1] Balick, B., & Frank, A. 2002, ARA&A, 40, 439

[2] Balick, B., Frank, A., Liu, B., et al. 2018, ApJ, 853, 168

[3] Bujarrabal, V., Castro-Carrizo, A., Alcolea, J., et al. 2001, A&A, 377, 868

[4] Castro-Carrizo, A., Neri, R., Bujarrabal, V., et al. 2012, A&A, 545, A1

[5] Castro-Carrizo, A., Bujarrabal, V., Neri, R., et al. 2017, A&A, 600, A4

[6] Corradi, R. L. M., Balick, B., & Santander-García, M. 2011, A&A, 529, A43

[7] de la Fuente, E., Trinidad, M. A., Tafoya, D., et al. 2022, PASJ, 74, 594

[8] Höfner, S. & Olofsson, H. 2018, The Astronomy and Astrophysics Review, 26, 1

[9] Kwok, S. 2000, The Origin and Evolution of Planetary Nebulae. Cambridge University Press

[10] Kwok, S., Purton, C. R., Matthews, H. E., & Spoelstra, T. A. T. 1985, A&A, 144, 321

[11] Lim, J., & Kwok, S. 2003, Symbiotic Stars Probing Stellar Evolution, 303, 437

[12] Livio, M. & Soker, N. 2001, ApJ, 552, 685

[13] Lykou, F., Chesneau, O., Zijlstra, A. A., et al. 2011, A&A, 527, A105

[14] Sahai, R., Morris, M., Sánchez Contreras, C., et al. 2007, AJ, 134, 2200

[15] Sahai, R. & Trauger, J. T. 1998, AJ, 116, 1357

[16] Sánchez Contreras, C., Báez-Rubio, A., Alcolea, J., et al. 2017, A&A, 603, A67

[17] Sánchez Contreras, C., Báez-Rubio, A., Alcolea, J., et al. 2019, A&A, 629, A136

[18] Ueta, T., Meixner, M., & Bobrowsky, M. 2000, ApJ, 528, 861